

# Iodide Ions Control Seed-Mediated Growth of Anisotropic Gold Nanoparticles

Jill E. Millstone, Wei Wei, Matthew R. Jones, Hyojong Yoo, and Chad A. Mirkin\*

*Department of Chemistry, Department of Materials Science and Engineering, and International Institute for Nanotechnology, Northwestern University, 2145 Sheridan Road, Evanston, Illinois 60208-3113*

*Received June 6, 2008*

## ABSTRACT

There are now a variety of preparatory procedures for nanoscale gold rods, triangular prisms, and spheres. Many of these methods rely on seed-mediated approaches with cetyltrimethylammonium bromide (CTABr) as a surfactant. Interestingly, seemingly similar preparatory procedures yield very different morphologies, and although there have been a variety of proposals regarding the importance of different steps in shape control, there is no self-consistent procedure that allows one to take one batch of spherical seeds and grow either rods, prisms, or larger polyhedra in a controlled manner. In this report, it is shown that CTABr, depending upon supplier, has an iodide contaminant (at a significant but varying level), which acts as a key shape-directing element because it can strongly and selectively bind to the Au (111) facet and favor the formation of anisotropic structures. Furthermore, by starting with pure CTABr and deliberately adjusting iodide concentration, one can reproducibly drive the reaction to predominantly produce one of the three target morphologies.

Efforts to generate nanoparticles of various sizes and shapes have produced a library of materials that allow one to observe the close relationship between nanostructure properties and physical architecture. These structure-dependent behaviors are of enormous interest for applications in photonics,<sup>1,2</sup> catalysis,<sup>3</sup> nanoelectronics,<sup>4</sup> and therapeutics.<sup>5-7</sup> For colloidal nanorods and nanoprisms made of gold, the preferred synthetic route is a seeding methodology. However, it is well-known that certain methods used to synthesize these particles are often irreproducible and difficult to control.<sup>8,9</sup> On the one hand, researchers have pointed to the importance of the surfactant (cetyltrimethylammonium bromide, CTABr), including surfactant concentration, counterion, alkane chain length, and even chemical manufacturer, on the yield and morphology of the resulting colloids.<sup>9-11</sup> On the other hand, researchers have also pointed to synthetic additives such as metal or halide ions as major factors in directing crystal growth.<sup>12-14</sup> However, there has not been a strong connection between these observations, and this has resulted in the development of numerous methods to access similar nanoparticle architectures.<sup>15-19</sup> These methods contain varied, sometimes contradictory, reports of the shape-directing factors in a given preparation.<sup>8,9,14,20</sup> For example, Sastry et al. report the suppression of gold nanoprism growth with the addition of iodide ion ( $I^-$ ) whereas Ha et al. report that

the presence of  $I^-$  promotes nanoprism formation.<sup>14,20</sup> In recent work, it was also shown that only CTABr obtained from certain manufacturers could produce nanorods, whereas other CTABr produced only pseudospherical particles.<sup>9</sup> In our work, we have observed both batch to batch CTABr sensitivity and an unexpected presence of  $I^-$  on the surface of gold nanoprisms (vide infra). Therefore, understanding the links between these seemingly disparate reports could provide valuable insight into the critical shape-directing factors involved in seed-mediated nanoparticle syntheses.

Herein, we report the controlled synthesis of gold nanorods, nanoprisms, and nanospheres under a unified framework that addresses previously reported results regarding the role of halide additives and the cationic surfactant, CTABr. The experimental approach focuses on understanding how to control shape using CTABr-based seeding methodology and is guided by the observation of  $I^-$  on Au nanoprisms using X-ray photoelectron spectroscopy (XPS). This observation is surprising since there is no apparent source of  $I^-$  anywhere in the synthesis (or other syntheses using similar approaches).<sup>9,11,13,21</sup> Interestingly, identical syntheses and seed particles could be used to form all three nanoparticle architectures, where the final shape was controlled by modulating only the iodide ion concentration in the reaction mixture. Importantly, the source of iodide in previous CTABr-based seed-mediated syntheses is now identified as the CTABr itself, which may explain the variability associ-

\* Corresponding author: fax, (+1) 847-467-5123; e-mail, chadnano@northwestern.edu.

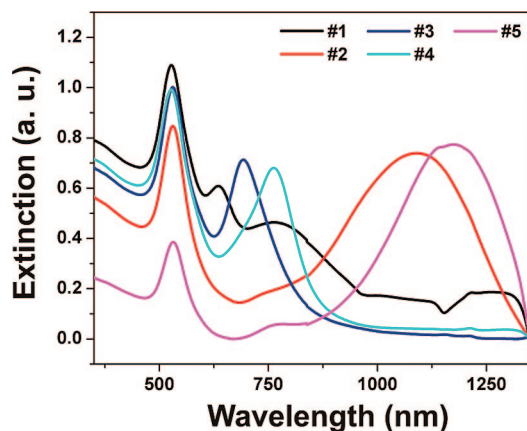


**Figure 1.** UV-vis-NIR spectra of nanoparticles produced using five different CTABr batches. Each CTABr was used as received from the manufacturer.

ated with its use.

In a typical seed-mediated gold nanoparticle synthesis, small gold seed nanoparticles ( $d \approx 4\text{--}6\text{ nm}$ ) are prepared by  $\text{NaBH}_4$  reduction of  $\text{HAuCl}_4$  and used in a subsequent three-step growth of these particles in an aqueous solution containing a capping agent (most commonly, CTABr), gold ions ( $\text{HAuCl}_4 \cdot 3\text{H}_2\text{O}$ ), reducing agent (ascorbic acid), and  $\text{NaOH}$  (to adjust pH and deprotonate ascorbic acid), together termed “growth solution”.<sup>16,21</sup> In order to understand the origin of the  $\text{I}^-$  in this synthesis, inductively coupled plasma mass spectrometry (ICP-MS) was used to analyze iodide concentration in the CTABr,  $\text{NaOH}$ ,  $\text{HAuCl}_4$ , ascorbic acid, sodium citrate, and  $\text{NaBH}_4$  used to prepare the nanoparticles (Supporting Information, Table S1). Only in the case of the CTABr was the presence of iodide detectable (ICP-MS detection limit for  $\text{I}^-$  is  $\sim 1\text{ ppb}$  under the conditions studied, see Supporting Information). We analyzed five additional batches of CTABr from various manufacturers with varying purities (Table S1). Interestingly, only certain CTABr batches contained  $\text{I}^-$ . Each of the five CTABr batches was used in repeated trials of the seed-mediated synthesis. With the CTABr that contained detectable traces of  $\text{I}^-$  (#2, #5), nanoprisms formed. For the other three CTABr samples, two produced various concentrations and distributions of nanorods, and one produced only pseudospherical nanoparticles (#1) (Figure 1). From these data, we hypothesized that the variation of seed-mediated syntheses based on CTABr may originate from variability in the observed iodide impurity.

In order to determine the shape-directing role of iodide in the formation of nanorods, nanoprisms, and nanospheres, CTABr (#2) was recrystallized using literature methods.<sup>22</sup> The recrystallized product was analyzed by ICP-MS and no  $\text{I}^-$  could be detected (#6). This purified CTABr was then used to analyze the *absolute*  $\text{I}^-$  concentrations necessary to produce a given shape morphology using seed-mediated methodology (it is important to note that others have concluded that use of the CTABr from different manufactures leads to different results, but the cause of this variability has yet to be identified<sup>10</sup>). In a typical experiment,  $\text{I}^-$  is introduced into the synthesis by adding aliquots of a  $\text{NaI}$  stock solution ( $0.1\text{ M}$ ) directly into the CTABr prior to

synthesis. Iodide concentrations of 0, 2.5, 5, 10, 50, and  $100\text{ }\mu\text{M}$  were investigated, and the same nanoparticle seed batch was used to initiate each reaction, in order to account for the effects of the seed nanoparticle morphology.

UV-vis-NIR spectra of the resulting solutions show a remarkable dependence of nanoparticle morphology on the presence of  $\text{I}^-$  (Figure 2A). With no  $\text{I}^-$  in solution, little anisotropic nanoparticle formation ( $<10\%$ ) is observed. However, with very low concentrations of  $\text{I}^-$  ( $2.5$  and  $5\text{ }\mu\text{M}$ ), a large population of nanorods can be observed ( $\sim 45\%$  yield before purification). As the concentration of  $\text{I}^-$  increases ( $>10\text{ }\mu\text{M}$ ), a mixture of nanoparticle morphologies is observed including rod, prism, and sphere morphologies. At  $50\text{ }\mu\text{M}$   $\text{I}^-$  concentration, nanoprisms form in high yield, as indicated by the strong dipole and quadrupole modes in the extinction spectrum ( $\sim 65\%$  yield before purification). However, at higher concentrations of  $\text{I}^-$  ( $>75\text{ }\mu\text{M}$ ), platelike growth continues but produces rounded, triangular and disklike particles. This analysis, based on the bulk characterization afforded by UV-vis-NIR spectroscopy, was confirmed by transmission electron microscopy (TEM) (Figure 2, panels B–D). Interestingly, these results were not dependent on the counterion of  $\text{I}^-$ . In addition to  $\text{NaI}$ ,  $\text{KI}$  and  $\text{LiI}$  produced similar results (Supporting Figure S2).

To analyze the role of  $\text{I}^-$  in these syntheses, we deposited nanoparticle solutions on silicon substrates for analysis by XPS. Interestingly, in all cases (both experiments using CTABr directly from the manufacturer and in experiments using purified CTABr and controlled introduction of  $\text{I}^-$ ), iodide was only observed on samples composed of nanoprisms; samples from rods and spheres did not exhibit detectable  $\text{I}^-$  signals by XPS (Figure 3). These results suggest that  $\text{I}^-$  is bound to the (111) crystal facet of the nanoprisms which compose their broad triangular faces.<sup>23</sup> It is well-known that halide ions adsorb on gold surfaces with binding energies that scale with polarizability ( $\text{I}^- > \text{Br}^- > \text{Cl}^-$ ) and crystal facet ( $(111) > (110) > (100)$ ).<sup>24</sup> In previous reports, it has been postulated that  $\text{I}^-$  preferentially binds to the (111) facet of a growing nanoparticle and prevents reaction at that surface.<sup>20</sup> However, reports describing this mechanism also pointed to competing shape-directing factors such as pH, temperature, and surfactant counterion and did not identify the original source of the  $\text{I}^-$ . We find that in standard CTABr-based, three-step, seed-mediated conditions,  $\text{I}^-$  is the dominant shape-directing moiety, more so even than the seed nanoparticle, as evidenced by the fact that the same batch of nanoparticle seeds can produce all three nanoparticle morphologies in high yield. This observation indicates that although there may be multiple seed morphologies within the single seed nanoparticle solution, their growth into anisotropic structures is not dictated by the initial structure alone. Otherwise, a single shape or shape distribution would be the preferred outcome over the others, regardless of additional reagents.

The dependence of nanoparticle morphology on iodide concentration may be understood based on the preferential adsorption of iodide on the (111) crystal facet of  $\text{Au}$ .<sup>24</sup> Without iodide, a CTABr bilayer is present on all surfaces

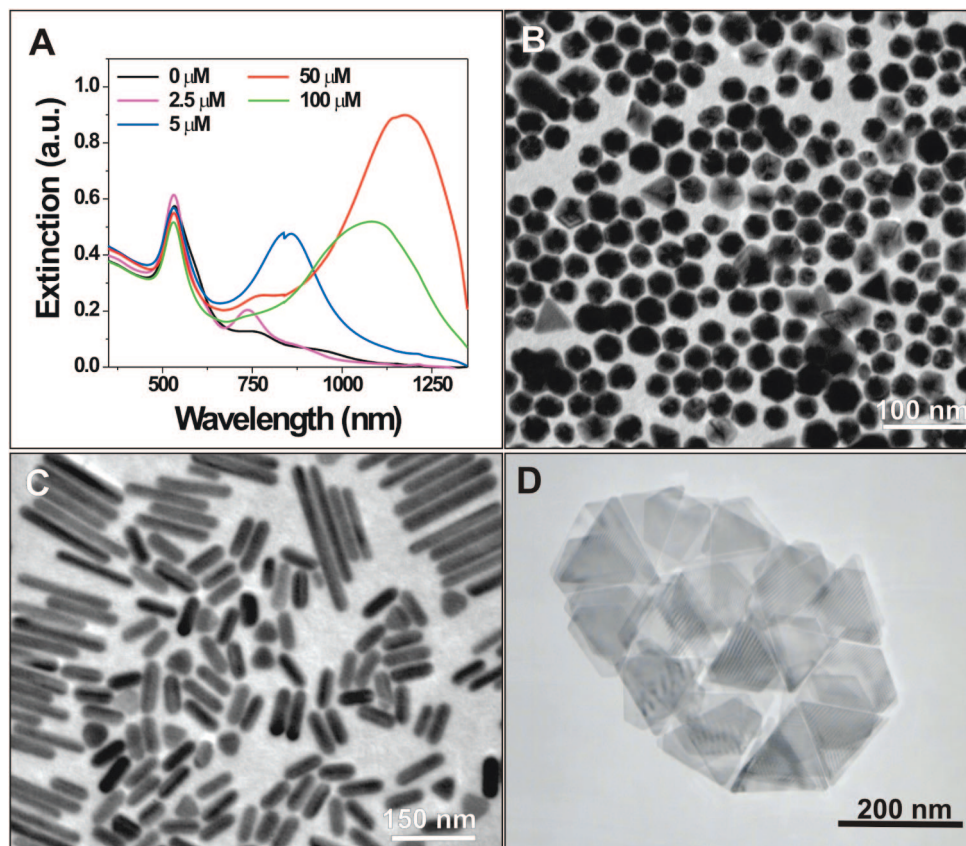


**Figure 2.** (A) UV-vis-NIR spectra of nanoparticles made using various concentrations of  $I^-$  and corresponding TEM images of (B) pseudospherical nanoparticles, (C) nanorods, and (D) nanoprisms.

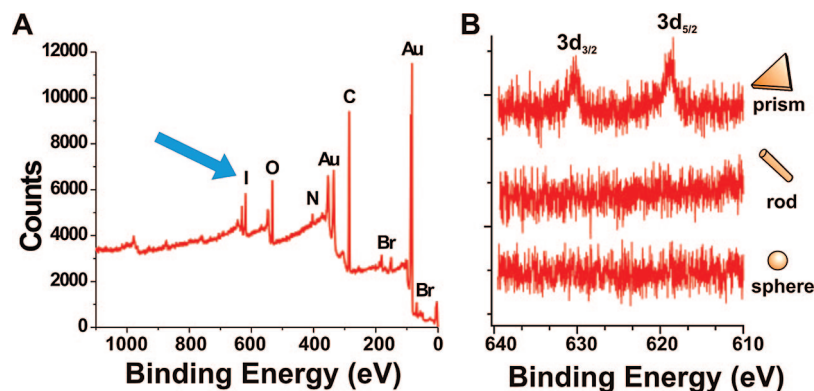


**Figure 3.** XPS spectra (A) of gold nanoprisms, arrow indicates  $I^-$  signal, (B) centered at binding energy of  $I^-$  and taken from nanoprisms, rods, and pseudospherical nanoparticles. Spectra indicate  $I^-$  only on nanoprisms.

due to electrostatic forces, which leads to a lack of preferential growth and an isotropic nanoparticle. With slightly increased iodide concentrations iodide adsorbs on the (111) crystal facet (at the ends of the rod), leaving the (110) and (100) (the long axis facets of the rod) open for the adsorption of a close-packed CTABr layer that can limit the reduction of gold ions at these sites.<sup>25,26</sup> This model is consistent with previous observations for rod formation and offers additional insight into why growth in the [111] direction can compete effectively to form nanorods.<sup>25,26</sup> It is also consistent with the observed XPS spectra of nanorods, which exhibit no detectable iodide from a well-dispersed nanorod sample with their long axis parallel to the substrate

(Figure 3B). Finally, at elevated concentrations of iodide, a layer of iodide is formed on the Au surface (as indicated by XPS,  $I_{3d} = 618.9$  eV).<sup>27</sup> This layer may promote nanoprism formation by allowing the chemical reactivity of the different crystal facets to dominate the growth processes with growth at the high energy side crystal facets favored.<sup>23</sup> Taken together, this model presents a series of competing factors for directing anisotropic nanoparticle growth where iodide plays the primary mediating role.

For these studies, the original conditions reported by others<sup>21,28</sup> and our group<sup>16</sup> have been used in an attempt to elucidate the shape-directing factors in CTABr-based seeding methodologies for the production of gold nanospheres,



nanorods, and nanoprisms. Importantly, these results demonstrate the critical role of iodide ion in these syntheses and the need for analytically pure CTABr, regardless of which morphology one wants to deliberately prepare. Finally, this work complements the growing body of work aimed at developing methods for preparing non-spherical noble metal nanostructures with control over critical architectural parameters.<sup>29</sup>

**Acknowledgment.** This work was supported by the ONR and AFOSR. C.A.M. is also grateful for an NIH Director's Pioneer Award and an NSSEF Fellowship from the Department of Defense. J.E.M. is grateful to Northwestern University for a Presidential Fellowship. M.R.J. is grateful to the National Science Foundation for a Graduate Research Fellowship. We thank David Giljohann for assistance with ICP-MS experiments.

**Supporting Information Available:** Full descriptions of materials and methods. This material is available free of charge via the Internet at <http://pubs.acs.org>.

## References

- (1) Fromm, D. P.; Sundaramurthy, A.; Kinkhabwala, A.; Schuck, P. J.; Kino, G. S.; Moerner, W. E. *J. Chem. Phys.* **2006**, *124*, 061101–1/4.
- (2) Maier, S. A.; Kik, P. G.; Atwater, H. A. *Appl. Phys. Lett.* **2002**, *81*, 1714–1716.
- (3) Narayanan, R.; El-Sayed, M. A. *Nano Lett.* **2004**, *4*, 1343–1348.
- (4) Gudiksen, M. S.; Lauhon, L. J.; Wang, J.; Smith, D. C.; Lieber, C. M. *Nature* **2002**, *415*, 617–620.
- (5) Hirsch, L. R.; Stafford, R. J.; Bankson, J. A.; Serksen, S. R.; Rivera, B.; Price, R. E.; Hazle, J. D.; Halas, N. J.; West, J. L. *Proc. Natl. Acad. Sci. U.S.A.* **2003**, *100*, 13549–13554.
- (6) Jain, P. K.; Lee, K. S.; El-Sayed, I. H.; El-Sayed, M. A. *J. Phys. Chem. B* **2006**, *110*, 7238–7248.
- (7) Rosi, N. L.; Giljohann, D. A.; Thaxton, C. S.; Lytton-Jean, A. K. R.; Han, M. S.; Mirkin, C. A. *Science* **2006**, *312*, 1027–1030.
- (8) Lofton, C.; Sigmund, W. *Adv. Funct. Mater.* **2005**, *15*, 1197–1208.
- (9) Smith, D. K.; Korgel, B. A. *Langmuir* **2008**, *24*, 644–649.
- (10) Gao, J. X.; Bender, C. M.; Murphy, C. J. *Langmuir* **2003**, *19*, 9065–9070.
- (11) Sau, T. K.; Murphy, C. J. *J. Am. Chem. Soc.* **2004**, *126*, 8648–8649.
- (12) Ha, T. H.; Koo, H. J.; Chung, B. H. *J. Phys. Chem. C* **2007**, *111*, 1123–1130.
- (13) Nikoobakht, B.; El-Sayed, M. A. *Chem. Mater.* **2003**, *15*, 1957–1962.
- (14) Rai, A.; Singh, A.; Ahmad, A.; Sastry, M. *Langmuir* **2006**, *22*, 736–741.
- (15) Ah, C. S.; Yun, Y. J.; Park, H. J.; Kim, W.-J.; Ha, D. H.; Yun, W. S. *Chem. Mater.* **2005**, *17*, 5558–5561.
- (16) Millstone, J. E.; Park, S.; Shuford, K. L.; Qin, L.; Schatz, G. C.; Mirkin, C. A. *J. Am. Chem. Soc.* **2005**, *125*, 5312–5313.
- (17) Murphy, C. J.; Gole, A. M.; Hunyadi, S. E.; Orendorff, C. J. *Inorg. Chem.* **2006**, *45*, 7544–7554.
- (18) Perez-Juste, J.; Pastoriza-Santos, I.; Liz-Marzan, L. M.; Mulvaney, P. *Coord. Chem. Rev.* **2005**, *249*, 1870–1901.
- (19) Shankar, S. S.; Rai, A.; Ankamwar, B.; Singh, A.; Ahmad, A. *Nat. Mater.* **2004**, *3*, 482–488.
- (20) Ha, T. H.; Koo, H.-J.; Chung, B. H. *J. Phys. Chem. C* **2007**, *111*, 1123–1130.
- (21) Busbee, B. D.; Obare, S. O.; Murphy, C. J. *Adv. Mater.* **2003**, *15*, 414–416.
- (22) Dearden, L. V.; Woolley, E. M. *J. Phys. Chem.* **1987**, *91*, 2404–2408.
- (23) Millstone, J. E.; Métraux, G. S.; Mirkin, C. A. *Adv. Funct. Mater.* **2006**, *16*, 1209–1214.
- (24) Magnussen, O. M. *Chem. Rev.* **2002**, *102*, 679–726.
- (25) Wang, Z. L.; Gao, R. P.; Nikoobakht, B.; El-Sayed, M. A. *J. Phys. Chem. B* **2000**, *104*, 5417–5420.
- (26) Nikoobakht, B.; El-Sayed, M. A. *Langmuir* **2001**, *17*, 6368–6374.
- (27) Bravo, B. G.; Michelhaugh, S. L.; Soriaga, M. P.; Villegas, I.; Suggs, D. W.; Stickney, J. L. *J. Phys. Chem.* **1991**, *95*, 5245–5249.
- (28) Brown, K. R.; Walter, D. G.; Natan, M. J. *Chem. Mater.* **2000**, *12*, 306–313.
- (29) (a) Bönnemann, H.; Richards, R. M. *Eur. J. Inorg. Chem.* **2001**, 2455–2480. (b) Burda, C.; Chen, X.; Narayanan, R.; El-Sayed, M. A. *Chem. Rev.* **2005**, *105*, 1025–1102. (c) Chen, S.; Carroll, D. L. *J. Phys. Chem. B* **2004**, *108*, 5500–5506. (d) Murphy, C. J.; Gole, A. M.; Hunyadi, S. E.; Orendorff, C. J. *Inorg. Chem.* **2006**, *45*, 7544–7554. (e) Wiley, B.; Sun, Y.; Chen, J.; Cang, H.; Li, Z.-Y.; Li, X.; Xia, Y. *MRS Bull.* **2005**, *30*, 356–361. (f) Tao, A. R.; Habas, S.; Yang, P. D. *Small* **2008**, *4*, 310–325. (g) Jin, R.; Cao, Y.; Mirkin, C. A.; Kelly, K. L.; Schatz, G. C.; Zheng, J. G. *Science* **2001**, *294*, 1901–1903. (h) Métraux, G. S.; Mirkin, C. A. *Adv. Mater.* **2005**, *17*, 412–415. (i) Xue, C.; Métraux, G. S.; Millstone, J. E.; Mirkin, C. A. *J. Am. Chem. Soc.* **2008**, *130*, 8337–8344. (j) Jin, R.; Cao, Y. C.; Hao, E.; Métraux, G. S.; Schatz, G. C.; Mirkin, C. A. *Nature* **2003**, *425*, 487–490.

NL8016253